Journal of Magnetic Resonance **147,** 110–115 (2000)
doi:10.1006/jmre.2000.2183, available online at http://www.idealibrary.com on IDEAL®

Synchronized Adiabatic Decoupling

Shanmin Zhang and David G. Gorenstein

Sealy Center for Structural Biology and Department of Human Biological Chemistry and Genetics, University of Texas Medical Branch, Galveston, Texas 77555-1157

Received March 30, 2000; revised July 21, 2000

A new decoupling scheme termed "synchronized adiabatic decoupling" is developed for use in the indirectly detected dimension. After each increment, the decoupling sequence is replaced by another one with different period T or different initial period T_{ini} so that sampling always occurs at the end of a complete decoupling period. The effects of J coupling are therefore completely averaged out for all data points. As a result, all decoupling sidebands disappear and the center band increases correspondingly. Since the synchronized adiabatic decoupling does not require conventional editing techniques to cancel the sidebands, it is useful in high-field gradient-enhanced multidimensional experiments with only a single scan per increment.

Key Words: **synchronized adiabatic decoupling; dynamic pulsing scheme; synchronized sampling; adiabatic decoupling; decoupling sidebands.**

INTRODUCTION

A RF pulse train, composed of repetitive pulses, is commonly employed in traditional spin decoupling (*1*). The quality of decoupling relies on how the pulses manipulate the spin interactions (J couplings for instance) under unfavorable conditions, such as large offset, inhomogeneity of the RF field, and low RF field strength.

For decoupling sequences with constant RF field strength f_1, such as MLEV-16 (*2*), WALTZ-16 (*3*), and GARP (*4*), the decoupling range Δf is proportional to f_1 or $f_{1\mathrm{rms}}$, while for adiabatic decoupling it is proportional to $f_{1\mathrm{rms}}^2$. To understand this, we consider first an arbitrary decoupling sequence with constant f_1. The rotational angle φ_i and axis n_i of the ith pulse in the sequence can be expressed as

$$\varphi_i = 2\pi\sqrt{f_1^2 + \Delta^2}\tau_i = 2\pi f_1\sqrt{1 + (\Delta/f_1)^2}\tau_i, \quad [1a]$$

$$n_{xi} = \frac{f_{1xi}}{f_1\sqrt{1 + (\Delta/f_1)^2}} = \frac{\cos(\theta_i)}{\sqrt{1 + (\Delta/f_1)^2}}, \quad [1b]$$

$$n_{yi} = \frac{\sin(\theta_i)}{\sqrt{1 + (\Delta/f_1)^2}}, \quad [1c]$$

$$n_{zi} = \frac{\Delta}{f_1\sqrt{1 + (\Delta/f_1)^2}}, \quad [1d]$$

where θ_i and τ_i are the phase and width of the ith pulse, and Δ is the offset. In Eq. [1a], $2\pi f_1\tau_i = \varphi_i$ ($\Delta = 0$) is the rotational angle under on-resonance conditions. When the RF field strength increases from f_1 to f_1' the pulse width must decrease accordingly from τ_i to τ_i' in order to keep the on-resonance rotational angle invariant, i.e.,

$$\varphi_i'(\Delta = 0) = \varphi_i(\Delta = 0) = 2\pi f_1'\tau_i' = 2\pi f_1\tau_i. \quad [2]$$

To keep both the rotational angle φ_i and the axis n_i (Eqs. [1a–1d]) invariant, the offset also needs to be increased accordingly from Δ to Δ' so that

$$\frac{\Delta'}{f_1'} = \frac{\Delta}{f_1}. \quad [3]$$

With proper settings of all of the pulse widths (Eq. [2]), the overall rotation introduced by successive rotations of all of the pulses or, equivalently, the decoupling effect for offset = Δ at RF field strength = f_1 is then the same as that for offset = Δ' at RF field strength = f_1' (Eqs. [1, 3]). It follows that the decoupling range Δf, which relates to the largest offset $\Delta_{\max}$ at which decoupling result is acceptable, is proportional to f_1, i.e.,

$$\Delta f = \Xi f_1, \quad [4]$$

where Ξ is a constant and is termed the figure of merit (*5–7*). For MLEV-64 (*8*), WALTZ-16, and GARP decoupling sequences, $\Xi \approx 2.2$, 2.2, and 4.8, respectively.

For adiabatic decoupling, however, both pulse phase and amplitude change during the frequency sweep to meet the condition of adiabatic inversion. As an example, we consider the offset-independent adiabatic decoupling (*9–11*). To derive such a decoupling sequence, it is sufficient to construct a decoupling sequence with the frequency sweep $f(t)$ and the amplitude $f_1(t)$ of the pulse satisfying the relationship of (*11*)

$$Q\frac{df(t)}{dt} = 2\pi f_1^2(t), \quad [5]$$

1090-7807/00 $35.00

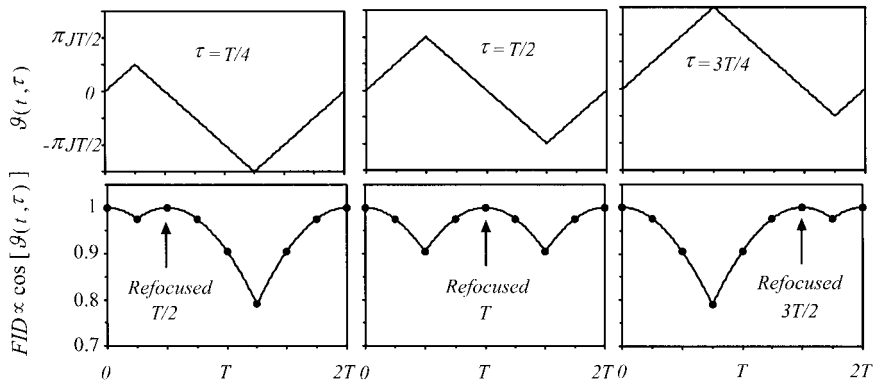

FIG. 1. Adiabatic decoupling phase $\vartheta(t, \tau)$ $(0 \le t \le 2T)$ for spin-flip occurring at $\tau = T/4$, $\tau = T/2$, and $\tau = 3T/4$, respectively (top), and their corresponding FID$(t) \propto \cos[\vartheta(t, \tau)]$ with a sampling dwell time of 0.5 ms (solid circles), where spin–spin relaxation is neglected. The FIDs are refocused at $T/2$, T, and $3T/2$ for spin inversion time $\tau = T/4$, $T/2$, and $3T/4$, respectively, and they are all refocused at $2T$.

where Q is the adiabaticity factor (*12*). Integrating both parts of Eq. [5] over the decoupling period, one obtains

$$\Delta f = \frac{2\pi}{Q} T f_{1\text{rms}}^2, \qquad [6]$$

where $f_{1\text{rms}} = (1/\sqrt{T})\sqrt{\int_0^T f_1^2(t)dt}$ is the root-mean-square value of the RF field strength. For constant RF field $f_1 = f_{1\text{rms}}$. A similar result as Eq. [6] was derived in Ref. (*6*).

For adiabatic decoupling, the figure of merit Ξ can be defined by the ratio of Δf to $f_{1\text{rms}}^2$, i.e.,

$$\Delta f = \Xi f_{1\text{rms}}^2. \qquad [7]$$

Comparing Eq. [7] with Eq. [6], we find that

$$\Xi = \frac{2\pi T}{Q} \qquad [8]$$

for the offset-independent adiabatic decoupling.

From Eqs. [4] and [6], one can see that adiabatic decoupling has a much higher decoupling efficiency than the traditional decoupling schemes with constant f_1, especially for broadband decoupling (*7, 11, 13–18*). As a matter of fact, the adiabatic decoupling has reached the highest decoupling index ($n = 2$), defined by the relationship of $\Delta f = \Xi(f_{1\text{rms}})^n$ (*18*). In addition, the adiabatic decoupling is much less sensitive to the inhomogeneity of the RF field, which is one of the most important factors to be considered in pulsed NMR.

In theory, spin interactions are minimized on average only at the end of decoupling periods for most decoupling schemes, i.e., the propagator, which governs the evolution of the density operator (*19, 20*),

$$L(T) = \mathbf{T} \exp\left[-i \int_0^T 2\pi(JI_zS_z + \Delta S_z + f_{1x}(t)S_x + f_{1y}(t)S_y)dt\right] \approx \mathbf{1}, \qquad [9]$$

over a certain range of Δ, where $\mathbf{T}$ is the Dyson time ordering operator.

In practice, however, sampling has to occur during the decoupling periods to meet the Nyquist frequency (*21*), especially for adiabatic decoupling with relatively long decoupling period. This nonsynchronized decoupling introduces deviations for those sampling points acquired not at a multiple of the decoupling periods ($2nT$ for adiabatic decoupling). Fortunately, these deviations will be corrected at the end of the decoupling periods (Fig. 1). Therefore, there is no long-term accumulation effect. Nevertheless, the periodic deviation causes severe sidebands in adiabatic decoupling and consequently reduces center band intensity. The sidebands can be cancelled effectively by properly editing the spectra obtained with different decoupling sequences or periods (*22, 23*). To eliminate the sidebands for $n = \pm 2$, a minimum of two scans are required and for $n = \pm 2$ and $n = \pm 4$ four scans are necessary. The intensity loss of the center band cannot be recovered by this method. The sidebands for $n = \pm 1$, $\pm 3, \ldots$, which have zero intensities under on-resonance decoupling conditions, can be minimized with proper initial adiabatic decoupling (*24*).

The decoupling sidebands can also be reduced significantly by varying decoupling periods within a single decoupling sequence to spread out the sidebands in a broad range (*25*). To make it effective, this decoupling usually requires a long cycle

time, making the scheme impractical in multidimensional NMR, especially in the indirectly detected dimension.

Sampling only at the end of decoupling periods is referred to as synchronized decoupling. It is limited only to a rather narrow spectral window for synchronized adiabatic decoupling in the directly detected dimension due to the long decoupling period. In the indirectly detected dimension, however, after each increment there will be an acquisition time and a relaxation delay of hundreds of milliseconds to seconds that is sufficient for substitution of a new sequence. In this way, each sampling point corresponds to its own decoupling sequence, which allows the data to be acquired at the end of a complete decoupling period. Consequently, all decoupling sidebands disappear and the center band increases correspondingly. To achieve this synchronized decoupling, each decoupling pulse may have different period T or different initial period T_{ini}.

PRINCIPLES

For adiabatic decoupling, a complete refocusing of J evolution, disregarding the offsets, actually occurs at $2T$ (Fig. 1) (*24*) assuming that the spin-flip during the frequency sweep is instantaneous (*22, 24*). The instantaneous spin-flip is equivalent to a strong π pulse applied at the time of spin inversion. The J evolution under the interaction of the adiabatic decoupling for a time of $2T$ can be described by the density operator formalism (*1, 24*),

$$\begin{aligned}\sigma(2T) &= e^{-i(2\pi JI_zS_z)(T-\tau)}e^{-i\pi S_x}e^{-i(2\pi JI_zS_z)T}e^{-i\pi S_x}e^{-i(2\pi JI_zS_z)\tau}I_x \\ &\quad\times e^{i(2\pi JI_zS_z)\tau}e^{i\pi S_x}e^{i(2\pi JI_zS_z)T}e^{i\pi S_x}e^{i(2\pi JI_zS_z)(T-\tau)} \\ &= e^{-i(2\pi JI_zS_z)(T-\tau)}e^{i(2\pi JI_zS_z)T}e^{-i(2\pi JI_zS_z)\tau}I_x \\ &\quad\times e^{i(2\pi JI_zS_z)(T-\tau)}e^{-i(2\pi JI_zS_z)T}e^{i(2\pi JI_zS_z)\tau} \\ &= I_x, \end{aligned} \quad [10]$$

where the first spin-flip occurs at τ and the second one at $T + \tau$. Equation [10] shows that the density operator $\sigma(2T)$ is refocused no matter when the S spin flips (Fig. 1). One can show that, at time T, $\sigma(T)$ is refocused only for on-resonance decoupling, with the S spin inverted in the middle of the pulse period ($\tau = T/2$). Synchronized decoupling, therefore, should occur at a multiple of $2T$ instead of T.

It follows from Eq. [10] that the density operator can be expressed as

$$\sigma(t, \tau) = I_x\cos[\vartheta(t, \tau)] + 2I_yS_z\sin[\vartheta(t, \tau)], \quad [11]$$

where the adiabatic decoupling phase $\vartheta(t, \tau)$ for $0 \le t \le 2T$ is defined as (*24*)

$$\vartheta(t, \tau) = \begin{cases} \pi Jt & 0 \le t \le \tau \\ \pi J(2\tau - t) & \tau \le t \le T + \tau, \\ \pi J(t - 2T) & T + \tau \le t \le 2T \end{cases} \quad 0 \le \tau \le T. \quad [12]$$

Regardless of the inversion time τ, $\vartheta(t, \tau)$ has a period of $2T$ and $\vartheta(0, \tau) = \vartheta(2T, \tau) = 0$ as shown in Fig. 1.

The free induction decay (FID) can be calculated directly from Eq. [11],

$$\begin{aligned}\text{FID}(t) &\propto \text{Tr}\{\sigma(t, \tau)(I_x + iI_y)\} \\ &\propto \cos[\vartheta(t, \tau)]. \end{aligned} \quad [13]$$

By varying the pulse period T, it is not difficult to design synchronized decoupling pulses except for a couple of initial sampling points with dwell time smaller than T. These initial points can be acquired with a strong decoupling pulse and short decoupling period (*26*). As an example, we consider a 2D experiment with a spectral width of 2 kHz in the indirectly detected dimension, which leads to a dwell time of 0.5 ms. The main adiabatic decoupling, referred to as main decoupling in the following, consists of a train of decoupling pulses with a period of $T = 2$ ms, which is too long for appropriate synchronized decoupling. To overcome the problem, two initial adiabatic decoupling pulses with the same period T_{ini} are inserted in the beginning of the decoupling pulse (*23*). As noted above, the two adiabatic decoupling pulses refocus the J phase evolution (or J modulation) of all decoupling offsets. For $T_{\text{ini}} = 1$ ms, the decoupling pulse $[T_{\text{ini}}][T_{\text{ini}}]$-main decoupling can be used as synchronized decoupling for sampling numbers of 1, 5, 13, 21, and $8n + 5 (n \ge 3)$, which corresponds to the sampling times of 0, 2, 6, 10, and $(8n + 4) \times 0.5$ ms, respectively. Similarly, for $T_{\text{ini}} = 1.25$ ms, the decoupling pulse can be used for sampling numbers of 6, 14, 22, and $8n + 6 (n \ge 3)$. Another six decoupling sequences with $T_{\text{ini}} = 1.5$, 1.75, 2, 2.25, 2.5, and 2.75 ms are needed for all the other sampling points as shown in Figs. 2 and 3.

EXPERIMENTAL

The main and all the initial adiabatic decoupling pulses are constructed as offset-independent adiabatic decoupling pulses based on Ref. (*11*) with a 34-kHz frequency sweep and a phase cycle of (0°, 150°, 60°, 150°, 60°) (*27, 28*) for the main decoupling. All the decoupling pulses have a WURST-2 shape $f_1(t) = f_{1\max}[1 - \sin^2(\beta t)]$, $-\pi/2 \le \beta t \le \pi/2$ (*16*). The main adiabatic decoupling has a period $T = 2$ ms, $f_{1\max} = 5.00$ kHz, and $f_{1\text{rms}} = 0.61\ f_{1\max} = 3.05$ kHz. To satisfy the condition of adiabatic inversion (*11, 12*), the RF strength for different initial periods T_{ini} is set according to the formula $f_{1\max}(T_{\text{ini}}) = \sqrt{T/T_{\text{ini}}}\, f_{1\max}$ (Eq. [6]), where T and $f_{1\max}$ are the period and field strength of the main adiabatic decoupling,

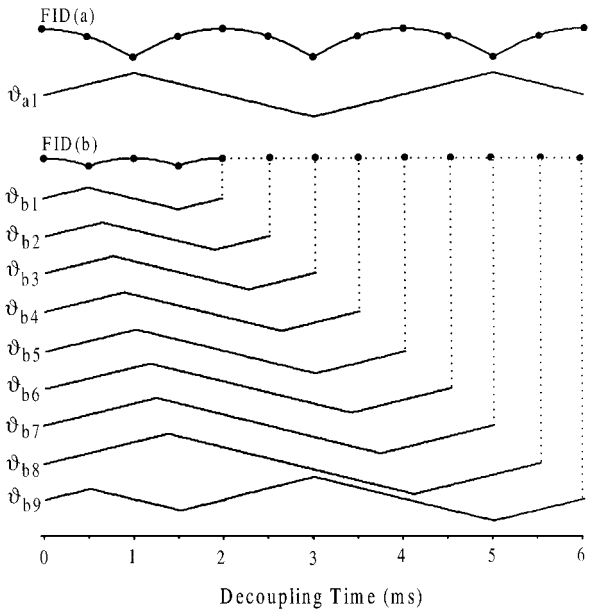

FIG. 2. Adiabatic decoupling with decoupling phase $\vartheta_{a1}(t, \tau = T/2)$ and its FID(a) $\propto \cos[\vartheta(t, \tau = T/2)]$ sampled at a dwell time of 0.5 ms (solid circles) (top), and synchronized adiabatic decoupling with different decoupling periods for different sampling points (bottom). The periods T related to their decoupling phases ϑ are $T_{a1} = 2$ ms, $T_{b1} = 1$ ms, $T_{b2} = 1.25$ ms, $T_{b3} = 1.5$ ms, $T_{b4} = 1.75$ ms, $T_{b5} = 2$ ms, $T_{b6} = 2.25$ ms, $T_{b7} = 2.5$ ms, $T_{b8} = 2.75$ ms. ϑ_{b9} has a $T_{ini} = 1$ ms and a main decoupling of $T = 2$ ms. The initial five data points of FID(b) are calculated from the phase ϑ_{b1}.

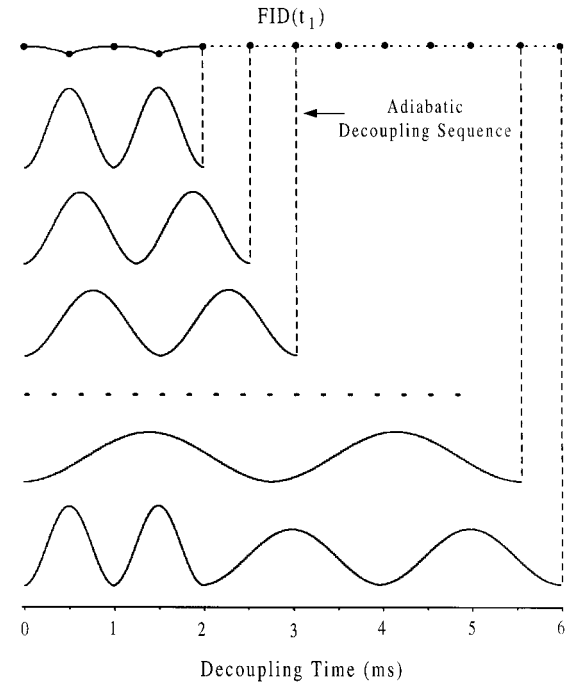

FIG. 3. The FID(t_1) sampled in synchronizing with the decoupling periods (except for several initial data points). To achieve synchronized decoupling different initial decoupling periods T_{ini} are used for different sampling points and, to achieve constant adiabaticity Q, different initial decoupling amplitudes A_{ini} are used for different periods T_{ini}. At $t_1 = 6$ ms, for example, the initial decoupling has a period $T_{ini} = 1$ ms and an amplitude $A_{ini} = \sqrt{2}A_{main}$.

respectively. For example, the RF strength for an initial decoupling with $T_{ini} = T/2$ is $f_{1max}(T/2) = \sqrt{T/(T/2)}f_{1max} = \sqrt{2}f_{1max}$.

The adiabatic inversion profiles of all the decoupling pulses are tested first using the Bloch equations (*29*, *30*) programmed in C language. The inversion profile provides a measure of the decoupling effects. An isolated *IS* spin-$\frac{1}{2}$ system is often assumed in adiabatic decoupling. In the case that the S spin is coupled to another spin S', ^{13}C–^{13}C coupling, for example, the effect of the S' spin is barely noticeable (see Figs. 4, 5, and 6). This lies in the factor that the S spin, unlike the decoupling with composite pulses, is inverted adiabatically by the effective field $f_{1eff}(t) = \sqrt{\Delta^2(t) + f_1^2(t)}$, which is usually much greater than the $J_{SS'}$ coupling between the S and S' spins. Therefore, the local field (at the S spin) created by the S' spin has little effect during the S spin inversion.

Experiments were performed on a Varian Unit-Plus 600-MHz NMR instrument with a Varian 5-mm HCN triple-resonance probe and a sample of ^{15}N- and ^{13}C-labeled (–COOH is unlabeled) *N*-acetylglycine in D_2O. A gradient COSY sequence is employed, detecting the methyl protons (diagonal peak) and decoupling the directly bonded ^{13}C.

Figure 4 shows the spectra of the methyl protons in the F_1 (indirectly detected) dimension from the traces of the gradient COSY spectra. Figure 4a is obtained with the main decoupling of $T = 2$ ms under on-resonance decoupling conditions. The sidebands for $n = \pm 2$ at ± 0.5 kHz appear as expected. Figure 4b is obtained using synchronized adiabatic decoupling (SAD) with a total of eight decoupling sequences of different initial

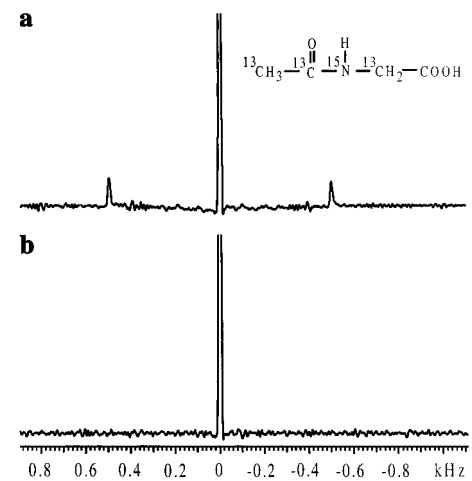

FIG. 4. Methyl ^1H spectra of *N*-acetylglycine in the F_1 dimension from the traces of two-dimensional gradient COSY spectra with a single scan per increment and with on-resonance ^{13}C adiabatic decoupling ($T = 2$ ms) (a) and with SAD (b). In the directly detected dimension, a WALTZ ^{13}C decoupling is used. A total of 128 increments and a spectral width of 2 kHz in the t_1 dimension are used in the experiments. The center peak is truncated at about the 31% level.

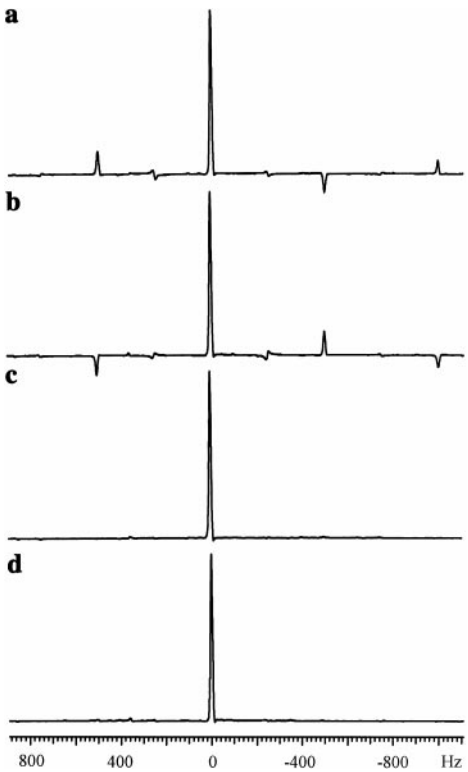

FIG. 5. Methyl ^{1}H spectra of *N*-acetylglycine in the F_1 dimension from the traces of two-dimensional gradient COSY spectra with a single scan per increment and with 4-kHz off-resonance ^{13}C adiabatic decoupling ($T = 2$ ms) (a and b) and with SAD (c and d). For both cases, no ^{13}C decoupling is applied in the directly detected dimension. The peak in the t_2 dimension is split into two (a and b and c and d) separated by the *J* coupling constant. The phases of the two peaks are different and are adjusted separately. A total of 256 increments and a spectral width of 2 kHz in the t_1 dimension are used in the experiments.

periods T_{ini} (Figs. 2 and 3). Since all the FID(t_1) data points are acquired under synchronized conditions (except for a few initial data points), the effects of the *J* coupling are completely removed. As a result, the sidebands disappear in the spectrum and the central band is enhanced about 5%, which is almost the sum of the intensities of the sidebands for $n = \pm 2$.

The spectra shown in Fig. 5 are obtained with 4-kHz off-resonance decoupling in the t_1 dimension and no decoupling in the t_2 dimension for both the main decoupling (Figs. 5a and 5b) and SAD (Figs. 5c and 5d). In the t_2 dimension each peak is split into two as plotted in Figs. 5a and 5b and 5c and 5d due to the *J* coupling. Both spectra in Figs. 5a and 5b show antiphase between the sideband number n and $-n$, which is contributed mainly from the sine modulation of the term $2I_yS_z\sin[\vartheta(t, \tau)]$ (Eq. [11]). The antiphase sidebands between Figs. 5a and 5b with the same sideband number n come mainly from the antiphase term $2I_yS_z\sin[\vartheta(t, \tau)]$ (Eq. [11]). All the sidebands, no matter in phase or antiphase, are effectively suppressed using SAD as shown in Figs. 5c and 5d. However, with proper decoupling in the t_2 dimension the antiphase sidebands, but not the in-phase sidebands, in t_1 dimension vanish as shown in Fig. 4.

Due to the insufficient memory of the acquisition system to hold all the adiabatic decoupling sequences, SAD is actually performed with eight COSY experiments, each with a different initial period T_{ini}, as discussed above. The final COSY data are constructed from the eight 2D data with a C program.

To perform the synchronized decoupling with a single experiment, one needs to either increase the memory of the acquisition system or develop a dynamic pulsing scheme (DPS) where the decoupling pulses, some other parameters, and even the whole pulse sequence can be changed after each scan.

As in the MAS experiment with synchronized sampling, SAD is limited to a rather narrow spectral width in the directly detected dimension, but DPS mentioned above can still be adapted to multidimensional experiments. After each scan the adiabatic decoupling pulse in the directly detected dimension can be replaced as well with a new one of different period *T*. In this way, the sidebands in the directly detected dimension will not be coherently added when performing Fourier transformation. Ideally, the reduction of sidebands will be $ni \times nt$ fold, where ni and nt are the number of increments and number of transients in a 2D experiment, respectively. The reduction of sideband intensities becomes even greater for higher dimensional experiments.

Figure 6 shows the spectra of the methyl protons in the F_2 (directly detected) dimension from the traces of the gradient HSQC spectra. Figure 6a is obtained with the main decoupling of $T = 2$ ms under on-resonance decoupling conditions. In addition to the sidebands for $n = \pm 2$ at ± 0.5 kHz, the sidebands for $n = \pm 1$ at ± 0.25 kHz appear as well. They are referred to as coherence sidebands and are caused mostly by

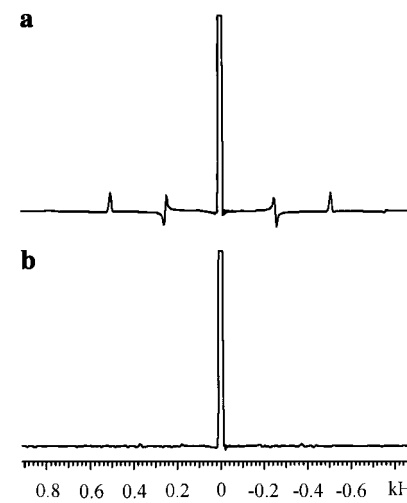

FIG. 6. Methyl ^{1}H spectra of *N*-acetylglycine in the F_2 dimension from the traces of two-dimensional gradient HSQC spectra with ^{13}C adiabatic decoupling ($T = 2$ ms) (a) and with DPS (b). A total of 64 increments and a spectral width of 4 kHz in the t_2 dimension are used in the experiments. The center peak is truncated at about the 16% level.

the antiphase and/or double-quantum coherences created prior to the adiabatic decoupling (*31*, *32*). Figure 6b is obtained with DPS of total 64 decoupling sequences of different periods T, from $1/T = 1000$ to 370 Hz in 10-Hz steps. After each t_1 increment a new decoupling sequence in the directly detected dimension is substituted with a frequency $f = 1/T$ as far apart as possible to the previous and the following ones in order to reduce interference. As expected, the sidebands are reduced significantly, but the center band remains the same since the sidebands are spread out in a broad range, resembling the scheme of varying the period in a single decoupling sequence. The advantage of this method over the varying period lies in that it can be used with short acquisition time in both the directly and the indirectly detected dimensions, especially for multidimensional experiments with insufficient sampling points.

DISCUSSION

Unlike any other decoupling schemes, SAD completely removes the effects of the J coupling in the indirectly detected dimension. As a consequence, all of the sidebands caused by the residual J modulation are removed without editing techniques and the center band is enhanced correspondingly. It is suitable for use in high-field gradient-enhanced multidimensional NMR experiments with only a single scan per increment.

This scheme of synchronization can also be used in other experiments where synchronized or stroboscopic sampling is required in the indirectly detected dimension but the pulse period is much longer than the dwell time. One of the experiments in solids is the separated local field experiment (*1*), where the period of the multiple pulse can be altered after each increment to meet the synchronized condition.

SAD can also be applied to homonuclear decoupling, ^{13}CO–$^{13}C_{\alpha}$ decoupling, for example. It is important to note that the sidebands, termed cyclic irradiation sidebands (*23*, *33*), are introduced mostly by direct irradiation of the decoupling RF field rather than by the modulation of the J coupling, and the cyclic irradiation sidebands have a fundamental frequency of $1/T$ rather than $1/2T$ (*24*, *33*). In addition, the Bloch–Siegert shift of all peaks will be introduced by the homonuclear decoupling (*23*, *33*–*37*), which can be removed by a compensating field and dilated evolution time (*23*, *33*).

ACKNOWLEDGMENTS

This research was supported by NIH (AI27744), NIEHS (ES06676), the Welch Foundation (H-1296), the Lucille P. Markey Foundation, and the Sealy and Smith Foundation. Building funds were provided by NIH (1CO6CA59098).

REFERENCES

1. R. R. Ernst, G. Bodenhausen, and A. Wokaun, "Principles of Nuclear Magnetic Resonance in One and Two Dimensions," Clarendon Press, Oxford, 1987.
2. M. H. Levitt, R. Freeman, and T. Frenkiel, *J. Magn. Reson.* **47,** 328 (1982).
3. A. J. Shaka, J. Keeler, T. Frenkiel, and R. Freeman, *J. Magn. Reson.* **52,** 335 (1983).
4. A. J. Shaka, P. B. Barker, and R. Freeman, *J. Magn. Reson.* **64,** 547 (1985).
5. A. J. Shaka and J. Keeler, *Prog. NMR Spectrosc.* **19,** 47 (1987).
6. Ē. Kupče, R. Freeman, G. Wider, and K. Wuthrich, *J. Magn. Reson. A* **120,** 264 (1996).
7. Z. Starčuk, Jr., K. Bartušek, and Z. Starčuk, *J. Magn. Reson. A* **107,** 24 (1994).
8. M. H. Levitt, R. Freeman, and T. Frenkiel, *Adv. Mag. Reson.* **11,** 47 (1983).
9. Ē. Kupče and G. Wagner, *J. Magn. Reson. B* **109,** 329 (1995).
10. Ē. Kupče and R. Freeman, *J. Magn. Reson. A* **118,** 299 (1996).
11. A. Tannús and M. Garwood, *J. Magn. Reson. A* **120,** 133 (1996).
12. Ē. Kupče and R. Freeman, *J. Magn. Reson. A* **117,** 246 (1995).
13. M. S. Silver, R. I. Joseph, C.-N. Chen, V. J. Sank, and D. I. Hoult, *Nature* **310,** 681 (1984).
14. J. Baum, R. Tyko, and A. Pines, *Phys. Rev. A* **32,** 3435 (1985).
15. M. R. Bendall, *J. Magn. Reson. A* **112,** 126 (1995).
16. Ē. Kupče and R. Freeman, *J. Magn. Reson. A* **115,** 273 (1995).
17. R. Fu and G. Bodenhausen, *J. Magn. Reson. A* **117,** 324 (1995).
18. S. Zhang, J. Wu, and D. G. Gorenstein, *J. Magn. Reson. A* **123,** 181 (1996).
19. U. Haeberlen and J. S. Waugh, *Phys. Rev.* **175,** 453 (1968).
20. M. Mehring, "High Resolution NMR Spectroscopy in Solids," Springer-Verlag, Berlin, 1976.
21. R. M. Bracewell, "The Fourier Transformation and Its Applications," McGraw-Hill, New York, 1965.
22. Ē. Kupče, *J. Magn. Reson.* **129,** 219 (1997).
23. S. Zhang and D. G. Gorenstein, *J. Magn. Reson.* **138,** 281 (1999).
24. S. Zhang and D. G. Gorenstein, *J. Magn. Reson.* **144,** 316 (2000).
25. T. Hwang, M. Garwood, A. Tannus, and P. C. M. van Zijl, *J. Magn. Reson. A* **121,** 221 (1996).
26. Ē. Kupče, R. Freeman, G. Wider, and K. Wuthrich, *J. Magn. Reson. A* **122,** 81 (1996).
27. R. Tycko, A. Pines, and R. Gluckenheimer, *J. Chem. Phys.* **83,** 2775 (1985).
28. T. Fujiwara and K. Nagayama, *J. Magn. Reson.* **77,** 53 (1988).
29. F. Bloch, *Phys. Rev.* **70,** 460 (1946).
30. S. Zhang and D. G. Gorenstein, *J. Chem. Phys.* **105,** 5659 (1996).
31. M. H. Levitt, G. Bodenhausen, and R. R. Ernst, *J. Magn. Reson.* **53,** 443 (1983).
32. M. R. Bendall and T. E. Skinner, *J. Magn. Reson.* **129,** 30 (1997).
33. S. Zhang and D. G. Gorenstein, *J. Magn. Reson.* **132,** 81 (1998).
34. F. Bloch and A. Siegert, *Phys. Rev.* **57,** 552 (1940).
35. S. Grzesiek and A. Bax, *J. Magn. Reson.* **96,** 432 (1992).
36. M. A. McCoy and L. Mueller, *J. Magn. Reson.* **98,** 674 (1992).
37. G. W. Vuister and A. Bax, *J. Magn. Reson.* **98,** 428 (1992).